Received: 16 October 2017 | Revised: 6 May 2018 | Accepted: 31 May 2018

DOI: 10.1002/hipo.22993

WILEY

RESEARCH ARTICLE

The ventral hippocampus is involved in multi-goal obstacle-rich spatial navigation

Marco Contreras[1] | Tatiana Pelc[1] | Martin Llofriu[2] | Alfredo Weitzenfeld[2] | Jean-Marc Fellous[1,3]

[1]Department of Psychology, University of Arizona, Tucson, Arizona

[2]Department of Computer Science and Engineering, University of South Florida, Tampa, Florida

[3]Department of Applied Mathematics, University of Arizona, Tucson, Arizona

Correspondence
Jean-Marc Fellous, University of Arizona, 1503 E University Boulevard, Room 312, Tucson AZ, 85721.
Email: fellous@email.arizona.edu

Funding information
National Science Foundation, Grant/Award Number: 1703340 and 1117388; Office of Naval Research Grants, Grant/Award Number: N000141310672; N000141512838 and N000141612829

Abstract

A large body of evidence shows that the hippocampus is necessary for successful spatial navigation. Various studies have shown anatomical and functional differences between the dorsal (DHC) and ventral (VHC) portions of this structure. The DHC is primarily involved in spatial navigation and contains cells with small place fields. The VHC is primarily involved in context and emotional encoding contains cells with large place fields and receives major projections from the medial prefrontal cortex. In the past, spatial navigation experiments have used relatively simple tasks that may not have required a strong coordination along the dorsoventral hippocampal axis. In this study, we tested the hypothesis that the DHC and VHC may be critical for goal-directed navigation in obstacle-rich environments. We used a learning task in which animals memorize the location of a set of rewarded feeders, and recall these locations in the presence of small or large obstacles. We report that bilateral DHC or VHC inactivation impaired spatial navigation in both large and small obstacle conditions. Importantly, this impairment did not result from a deficit in the spatial memory for the set of feeders (i.e., recognition of the goal locations) because DHC or VHC inactivation did not affect recall performance when there was no obstacle on the maze. We also show that the behavioral performance of the animals was correlated with several measures of maze complexity and that these correlations were significantly affected by inactivation only in the large object condition. These results suggest that as the complexity of the environment increases, both DHC and VHC are required for spatial navigation.

KEYWORDS

longitudinal axis, multiscale representations, spatial navigation, ventral hippocampus

1 | INTRODUCTION

Converging evidence indicates that distinct functions may be performed by different sub-regions of the hippocampus (HC) along its dorsoventral axis (also referred to as septotemporal or longitudinal axis). The consensus is that the dorsal hippocampus (DHC) supports spatial learning and that the ventral hippocampus (VHC) is primarily involved in emotional and motivational processes (Fanselow & Dong, 2010; Harland, Contreras, & Fellous, 2017; Poppenk, Evensmoen, Moscovitch, & Nadel, 2013; Strange, Witter, Lein, & Moser, 2014).

Previous studies have shown that DHC, but not VHC lesions, impair spatial learning (Gaskin, Gamliel, Tardif, Cole, & Mumby, 2009; Moser, Moser, & Andersen, 1993), whereas VHC, but not DHC lesions, reduce anxiety and fear expression (Bannerman et al., 2003; Deacon, Bannerman, & Rawlins, 2002; Richmond et al., 1999). However, other studies have shown that the VHC may be crucial in goal-oriented learning in mice navigating a water maze (Ruediger, Spirig, Donato, & Caroni, 2012) and that it may also be necessary for learning and recall in a similar task in rats (de Hoz, Knox, & Morris, 2003; de Hoz & Martin, 2014; Ferbinteanu, Ray, & McDonald, 2003; Loureiro et al., 2012). Furthermore, lesions made to the intermediate HC in rats impair the performance in a rapid place-learning task in the water maze (Bast, Wilson, Witter, & Morris, 2009). VHC interacts bidirectionally with the medial prefrontal cortex, an area well known to

contribute to decision making and working memory in general and to spatial navigation tasks in particular (De Saint Blanquat et al., 2013; Hok, Chah, Save, & Poucet, 2013). The findings from these studies point to a more complex functional organization of the dorsoventral axis than the traditional dichotomous dorsal–ventral differentiation (Nadel, 1968), a suggestion that now finds ample support (Fanselow & Dong, 2010; Risold & Swanson, 1996; Strange et al., 2014). New tasks and paradigms are however still needed to study the dorsal–ventral interactions specifically, especially in the context of spatial navigation.

The dorsal and ventral hippocampus poles differ in anatomical connectivity (Ciocchi, Passecker, Malagon-Vina, Mikus, & Klausberger, 2015; Kerr, Agster, Furtak, & Burwell, 2007), distribution of neuromodulator receptors (Amaral & Kurz, 1985; Gasbarri, Verney, Innocenzi, Campana, & Pacitti, 1994), gene expression (Thompson et al., 2008), and physiological properties of neurons (Dougherty, Islam, & Johnston, 2012; Giocomo & Hasselmo, 2008; Giocomo & Hasselmo, 2009). Seminal studies have established that dorsal place cells possess small, stable, and spatially selective firing fields while ventral cells have larger, less stable, and less spatially selective fields (Jung, Wiener, & McNaughton, 1994; Kjelstrup et al., 2008; Maurer, Vanrhoads, Sutherland, Lipa, & McNaughton, 2005). The spatial scale representation along the longitudinal axis of HC expands from less than 1 m near the dorsal pole to about 10 m near the ventral pole (Kjelstrup et al., 2008). The difference of scale may however not affect spatial resolution at the network level (Keinath et al., 2014).

How the spatial representation at multiple scales along the dorsoventral axis of the HC is used for navigation remains poorly understood. This knowledge gap is due in part to the fact that the vast majority of behavioral work on the contribution of DHC and VHC to spatial navigation used relatively simple tasks in small and simple environments. It is unclear whether using multiple scales of spatial representation truly matters in such cases. It is likely however, that complex tasks involving multi-goal learning and obstacles of different size (spatial frequency) would require an assessment of space at multiple scales. Interestingly, it has been reported in humans, that the level of complexity (number of distinct paths within the maze) of a virtual environment engaged the anterior part (rodents VHC), but not posterior segment (rodents DHC) of the hippocampus. In contrast, variation in the size of the environments engaged the posterior, but not anterior hippocampus (Baumann & Mattingley, 2013). While suggestive, these imaging studies did not offer the type of detailed mechanistic insights possible with animal studies.

We study whether rodent DHC and VHC are engaged in spatial navigation in a regular-size complex environment featuring many choice points and obstacles. We report that the inactivation of DHC or VHC impaired the performance in memory-guided spatial navigation in obstacle-rich environments but not in obstacle-free environments. These findings suggest that spatial navigation in a complex environment requires a greater involvement of the hippocampal circuitry than previously thought, especially at the ventral levels. These studies prompt the design of new computational models to further analyze the impact of DHC–VHC interactions in biologically inspired mobile robots.

2 | METHODS

2.1 | Animals

Thirteen Brown Norway (7–8 months old) and six Long Evans (3–5 months old) adult male rats were used in this study. Animals were housed individually on a reversed 24-hr light/dark cycle, with regular chow and water ad libitum. During testing, animals were food restricted to about 85% of their ad libitum weight and the experiments were conducted in the dark (active) phase of the cycle. The number of animals in each experiment and condition is noted in the figures. All procedures described below were approved by the IACUC of the University of Arizona and followed NIH guidelines.

2.2 | Apparatus

The apparatus used was an open-field circular arena of 1.5 m diameter enclosed by a 30.5 cm high wall (Jones, Bukoski, Nadel, & Fellous, 2012). Eight feeders were positioned at equidistant locations around the periphery. Each feeder was attached to a sugar water dispenser and a white light emitting diode (LEDs). Single drops of sugar water (0.2 g/mL) were used as a reward. The onset of LED illumination was used as a cue in the learning phase and it could be delayed to assess whether rats went to the feeders using memory alone in the memory test of the learning phase and during the recall phase (Figure 1a). An overhead video camera was used to track the movement of the animals (20–25 fps), and the feeders and lights were automatically controlled by custom-written software (LabView, National Instrument, Austin, TX). During the experiments, the spatial context was manipulated by replacing and repositioning one of two local cues located on the walls of the arena (intra-maze cues) and one large global cue located on the wall of the room (extra-maze cue). One local cue was kept constant across the conditions within an experiment so that the rats could orient themselves on the table despite contextual changes. All experiments were conducted in dim light (~0.5 Lux).

LEGO blocks were used to build 16 small (19 × 13 × 3 cm) or four (19 × 52 × 3 cm) large obstacles which were placed on the open-field in a pseudorandom position during the recall phase of the experiment.

2.3 | Intracerebral cannulation and injections

Following the completion of their final pretraining session, animals were anesthetized with 1.5–2.5% isoflurane at a flow rate of ~3.0 L/min, placed in a stereotaxic apparatus and implanted with two stainless steel guide cannulae (Plastic One) into DHC (3.8 mm posterior to bregma, 2.5 mm lateral to midline, and 2.5 mm below the skull) or VHC (5.2 mm posterior to bregma, 5.0 mm lateral to midline, and 3.2 mm below the skull). Cannulae were fixed to the skull with dental acrylic and four stainless steel microscrews. Occluders were inserted into the cannulas. Body temperature was maintained at 35 °C using a temperature-controlled heating pad. Following surgery, rats were injected with Carprofen (Rimadyl, 3 mg/kg SC) and antibiotic (Sulfamethoxazole and Trimethoprim oral suspension, Hitech Pharmacal, 16 mL/200 mL antibiotic/water) was administered in drinking

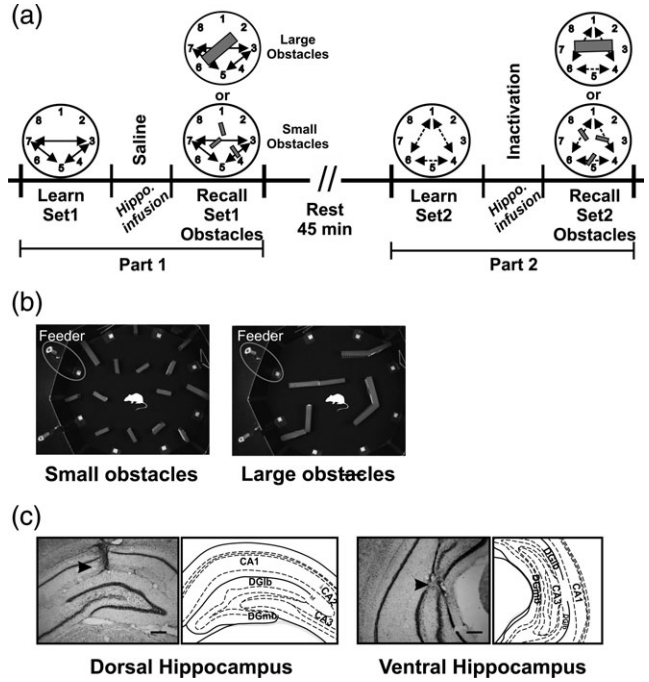

FIGURE 1 Behavioral protocols and histology. (a) Timeline of the experiments. Rats had to memorize the locations of a set of rewarded feeders, and recall these locations in the presence of small or large obstacles, or no obstacles (not shown). Animals received 2.5% bupivacaine hydrochloride or saline delivered in the ventral or dorsal hippocampus just before recall. (b) Examples of the overhead camera view of the small (left) and large (right) obstacles positioned on the maze. (c) Nissl stain of representative coronal hippocampal sections. Injection cannula tracts targeted to the dorsal (left) and ventral (right) hippocampus are indicated by black arrowheads. Injections were bilateral (only one side is shown for clarity). Scale bars = 300 μm

water for 5 days postsurgery. All rats were allowed to recover for at least 5 days before behavioral testing.

Rats received bilateral infusion of bupivacaine hydrochloride (1 μL/side. 2.5% dissolved in 0.9% sterile saline solution) or vehicle (0.9% sterile saline) on each experimental day, after learning and before the recall session (Figure 1a). Bupivacaine, a sodium channel blocker, was chosen because it has a fast induction time, a duration of effect up to 1 hr (Farnham & Pilowsky, 2009), and a smaller functional spread than muscimol (Edeline, Hars, Hennevin, & Cotillon, 2002). Electrophysiological evidence indicates that the spread of neural inactivation following the intracerebral injection of an amino-amide anesthetic may closely conform to the spherical volume Equation ($V = 4/3pi[r]^3$; Tehovnik & Sommer, 1997). Based on this analysis, the functional spread of 1 μL of bupivacaine would be about 0.62 mm. Considering the coordinates of the targeted injection site for the DHC and VHC, the infusions are restricted to the hippocampus. This type of reversible local anesthetic has been previously used in the inactivation of the hippocampus (Gabriele & Packard, 2006; Schroeder, Wingard, & Packard, 2002). The injection cannulae were coupled to a 10 μL Hamilton syringe by a polyethylene tubing (inner diameter 1.27 mm; Plastics One) filled with bupivacaine or vehicle and inserted into the guide cannula after removing the occluders. Infusions were done in awake rats (Brown Norway's) or under brief isoflurane anesthesia (1–0.7% in oxygen at a flow rate of ~3.0 L/min; <15 min; Long Evans), and lasted about 1 min on each side; the injection cannula was left in place for 2 min to allow for adequate diffusion of the substance, and then slowly removed and the occluders reinserted. Because the Long Evans rats showed more locomotor activity than Brown Norway rats during the infusion procedure, we decided to perform the infusions on that group under brief and light isoflurane anesthesia to ensure the proper delivery of the drug. It has been reported that isoflurane anesthesia could produce cognitive impairments in human and rodents. However, these impairments were observed with longer exposures (>2 hr) than those used here (<15 min), and were controlled for here using saline injections (Callaway, Jones, & Royse, 2012; Carr, Torjman, Manu, Dy, & Goldberg, 2011).

For subjects receiving infusions into DHC, the injection cannulae (33 gauge, Plastics One) protruded 1 mm from the tip of the guide cannulae. For subjects receiving infusions into VHC, the injection cannulae (33 gauge, Plastics One) protruded 2.8 mm from the tip of the guide cannulae.

2.4 | Behavioral training and test procedures

Rats were first habituated to the room and to sugar water. Animals were then pretrained to go to a blinking feeder light activated in random order to get a reward (Jones et al., 2012; Jones, Pest, Vargas, Glisky, & Fellous, 2015). After recovery from surgery, rats were briefly retrained on this random task before the start of the experiments.

Each experimental day consisted of two parts which differed in local and distal visual cues, set of feeders (e.g., Set 1 = 3,5,7; Set 2 = 1,4,6), drug infusion (bupivacaine or saline), and the recall conditions (large obstacles, small obstacles, and no obstacles). The experimental conditions were counterbalanced between days and rats. Both parts started with a learning phase (no obstacles) followed by an infusion and then a recall phase with or without obstacles (Figure 1a). The two parts of the experiment were separated by a 45-min period during which the rat rested on an opaque towel-lined pedestal in the center of the maze.

The learning phase started with a period during which the rats were cued by blinking lights to run to three predetermined feeders (set of feeders) in randomized order. After they received 100 rewards, the light cues were delayed by 15 s (timeout), and the rats visited the correct feeders using the memory of previously visited goal locations alone (memory test of the learning phase). The delay was reset if the rat reached the feeder within 15 s (a rat typically travels between two feeders in <6 s, so the delay allowed enough time to reach the feeders without cue), and the next light cue was again delayed by 15 s. The learning criterion was reached when the rats visited 15 correct feeders in a row, with no more than two timeouts. To keep the rats motivated while minimizing the amount of reinforcement, a correct feeder was rewarded 50% of the time after having visited a different correct feeder. Once the criterion was reached, the learning phase was completed and the rat was placed on the pedestal surrounded by an opaque cylinder (25 cm diameter) for 10 min.

After 10 min of the rest period, while the rat was still in the cylinder, small or large obstacles (Figure 1b, left and right panel respectively) were placed on the maze. Rats were then infused with bupivacaine or saline into the target regions and 45 s (nonanesthetized animals) or 10 min (anesthetized animals) later, the recall session started.

The recall phase was conducted without blinking lights, as in the memory test of the learning phase, in the presence of large or small obstacles. Therefore, to reach the rewards locations during the recall, the rats had to navigate using their memory of previously visited goal locations. The recall terminated when rats reached the same criterion as during learning. Once the criterion was reached, the rats were placed on the pedestal surrounded by the opaque cylinder for 10 min. Each day included one bupivacaine and one saline injection, pseudo-randomly ordered. Control experiments were performed in the same way except that the recall session was conducted without obstacles.

2.5 | Histology

Rats were perfused transcardially with 200 mL of cold and heparinized 0.9% saline followed by 250 mL of 4% paraformaldehyde in 0.1 M phosphate buffer. The brains were removed and cryoprotected in 30% sucrose and 0.02% sodium azide solution. The brains were frozen and 50-μm coronal sections were acquired with a cryostat (Leica). The brain sections were then stained with cresyl violet and the location of the injection tips was determined using a light microscope (Figure 1c).

2.6 | Data collection, behavioral, and complexity measurements

The (X,Y) coordinates of the rats during recall sessions were tracked and saved for analysis. Custom Matlab code was used to extract total time of the recall session, velocity profiles, movement time, number and location of stops, tortuosity of the trajectories, and stops at the correct and incorrect feeders. Sessions in which rats failed to reach the learning criterion were excluded from the analysis.

Several behavioral measures of the paths taken by the animals were computed. For simplicity, we present a subset of these measures. A *stop at a nontarget* is defined as a bout of tracking data of at least 0.5 s at a velocity of less than 3 cm/s within 11 cm of a nontarget feeder. During the recall, the *total distance traveled* is computed in meters as the sum of all path segments (from a valid target to another valid target) during which the animal was moving (velocity > 3 cm/s) until the recall criterion was reached. The number of *monotonous paths* was computed as follows. First, for each target-to-target segment, the instantaneous curvatures at every point were computed (Machine Vision package, LineCurvature2D.m, DJ Kroon). The curvatures were smoothed using a window of a width set to 10% of the segment. For each segment, the number of left turns was defined as the number of curvature clusters larger than a fixed value CTh (Curvature Threshold. Here CTh = 0.015 m^{-1}) and the number of right turns as the number of curvature clusters smaller than −CTh. A segment was considered monotonous if it had no detectable curvatures (all curvatures less than CTh in absolute value), only right curvatures or only left curvatures. This measure was taken as indicative of a stereotypical bout of navigation. All values for thresholds and fixed algorithm parameters mentioned above were determined empirically using at least three saline and three bupivacaine sessions from different rats and were kept identical for all analyses.

For each target-to-target segment, *tortuosity* is defined as the arc-chord ratio (length of segment traveled divided by the length of the target-to-target direct chord) and is always >1.

As there are no agreed-upon measures of maze complexity, we propose several measures (Figure 6). After each experiment, an overhead picture of the maze was taken (Figure 1b). The obstacles (polygons), reward locations (points) and maze walls (polygon) were digitized. Obstacle *Density* is defined as the fraction of the area occupied by the obstacles (unit: %) and captures the overall clutter of the maze. Figure 6a shows two maze layouts with low (left) and high (right) obstacle density. *Straight-path Complexity* was defined as the average number of obstacles encountered on the way (straight line) from i to j, for each pair of rewarded targets (i,j). This quantity measures the amount of impediment from one reward location to another. Figure 6b shows two mazes of equal obstacle density, low (left: 1/3 = 0.33) and high (right, 3/3 = 1.0) straight-path-complexities. *Line-of-Sight Complexity* (unit: %) was defined as follows: For each pair of rewards i and j, a straight line was drawn. This line was discretized in 21 equidistant segments. For each point, a line was further drawn to the third reward k. If this line met an obstacle, it was labeled "obstructed". Line-of-sight complexity was computed as the overall fraction of obstructed paths for a given set of reward locations (i.e., for three rewards, 20 lines of sights: Number of obstructed paths/60). This measure captures the extent to which other rewards are visually available for future path planning, as the animal moves from one reward to another. Figure 6c illustrates the measure for eight equidistant segments on one or the three target-to-target paths for clarity. The left maze had low complexity (2/7 = 0.28), the right maze had high complexity (4/7 = 0.57). Both mazes had the same density and same straight-path complexity.

The statistical differences between the different types of injections and experimental conditions were analyzed using either Wilcoxon Signed-Ranks test or Mann–Whitney *U* test. Linear regression analyses were performed to determine Pearson correlation coefficients (r) and coefficient of determination (r^2) between navigational performance and maze complexity. Fisher's *r*-to-*Z* transformations compared the correlation coefficients between saline and bupivacaine in small and large obstacles conditions. In all figures, significance levels were set to <0.05 (*) and < 0.01 (**).

3 | RESULTS

3.1 | Histology

Representative photomicrographs and schematics illustrating the injection cannula placements in the hippocampus are shown in Figure 1c. The tip of the injection cannula tracks was located within the target regions (i.e., DHC and VHC) bilaterally for all rats whose data were included in data analyses. The histological analysis of the

distribution of cannula placements in the DHC confirmed that the injection cannula tracks were located mainly in the CA1 area and the dentate gyrus, whereas the cannula tips in the VHC were located in the CA1-CA3 areas and the dentate gyrus. Considering that the spread of neural inactivation following a 1 μL diffusion of bupivacaine would be ~0.62 mm, it is reasonable to conclude that the CA3 area in the DHC may also have been affected by bupivacaine. The data from two animals (two Long Evans rats) were excluded from analysis because of misplaced injection sites.

3.2 | Experiment 1: effect of dorsal or ventral hippocampus inactivation on memory-guided navigation in obstacle-free environments

The purpose of this experiment was to evaluate the effect of the DHC or VHC inactivation on memory-guided spatial navigation in an obstacle-free environment (simple environment). Rats learned two sets of feeders (Set1 and Set2) on the same experimental day (Figure 1a). Following learning, we performed the infusion of saline or bupivacaine into DHC or VHC and the recall was conducted in an obstacle-free environment. Figure 2a shows representative examples of rat trajectories during recall in the obstacle-free condition after saline (Figure 2a left) or bupivacaine (Figure 2a right) infusion in DHC (top) or VHC (bottom). Figure 2b shows the number of times rats stopped at feeders that were not part of the learned set (nontargets). Figure 2c shows the number of timeouts required to reach the same criterion as in the learning phase. Figure 2d shows the average number of monotonous segments per session. Figure 2e shows the total distance traveled by the rats before reaching the learning criterion. No significant differences between saline and bupivacaine infusions across all measures were detected for DHC (Wilcoxon Signed-ranks test; stops nontarget, $Z = -0.40$, $p = .69$; timeouts, $Z = -1.12$, $p = .26$; monotonous segments, $Z = -0.78$, $p = .44$; distance traveled, $Z = -1.68$, $p = .93$) or VHC (Wilcoxon Signed-ranks test; stops nontarget, $Z = -1.16$, $p = .25$; timeouts, $Z = -0.63$, $p = .53$; monotonous segments, $Z = -0.19$, $p = .85$; distance traveled, $Z = -0.77$, $p = .44$). Bupivacaine has proven to be a reliable pharmacological agent for temporarily inactivating a number of brain structures including the hippocampus (Gabriele & Packard, 2006). Additional analyses revealed that the effects of VHC inactivation were not significantly different from those observed with DHC inactivation for all path measures (Mann–Whitney test; saline, stops nontarget, $U = 29.5$, $p = .11$; timeouts, $U = 49$, $p = .97$; monotonous segments, $U = 343$, $p = .13$; distance traveled, $U = 38$, $p = .62$; bupivacaine, stops nontarget, $U = 47.5$, $p = .63$; timeouts, $U = 46$, $p = .57$; monotonous segments, $U = 422.5$, $p = .38$; distance traveled, $U = 29$, $p = .76$). These results indicate that the inactivation technique we used did not impair the navigation performance or the memory for rewarded locations in this simple task in which no obstacle was present.

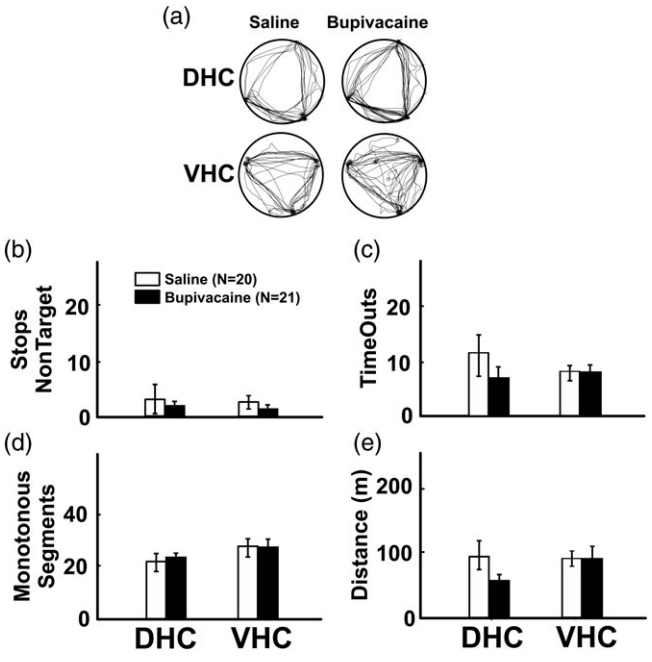

FIGURE 2 Reversible inactivation of the VHC or DHC does not affect spatial navigation in obstacle-free environments. (a) Representative rat trajectories during recall after saline or bupivacaine infusion in the DHC (upper) or VHC (lower). (b) Number of times rats stopped at nontargets. (c) Number of timeouts required to reach the recall criterion. (d) Average number of monotonous segments. (e) Total distance traveled before reaching recall criterion. *N* indicates the number of sessions. DHC group, $n = 8$ rats. VHC group, $n = 9$ rats

3.3 | Experiment 2: effect of dorsal or ventral hippocampus inactivation on memory-guided navigation in an environment with large obstacles

The purpose of this experiment was to evaluate the effect of DHC or VHC inactivation on spatial memory recall in an environment containing large obstacles. Rats were treated as described in Experiment 1 except that the recall test was performed in the presence of large obstacles. Figure 3a shows representative rat trajectories during recall in the large obstacle condition after saline (left) or bupivacaine (right) bilateral infusion into the DHC (top) or VHC (bottom). Bupivacaine infusion into the VHC, but not in the DHC significantly increased the number of times rats stopped at the nontarget feeders when compared to saline (Figure 3b, Wilcoxon Signed-ranks test, DHC, $Z = -1.93$, $p = .054$; VHC, $Z = -2.80$, $p = .005$). There was no significant difference in the number of stops between DHC and VHC inactivation (Mann–Whitney test, saline $U = 58.5$, $p = .17$; bupivacaine, $U = 53.5$, $p = .12$). In contrast, bupivacaine infusion in the DHC, but not in the VHC or saline infusion into the DHC, increased the average number of monotonous segments, indicating that the animals did not circumnavigate the obstacles as often as in the saline condition (Figure 3d, Wilcoxon Signed-ranks test, DHC, $Z = -2.28$, $p = .02$; VHC, $Z = -1.07$, $p = .28$). There was no significant difference in the number of monotonous segments between DHC and VHC inactivation (Mann–Whitney test, saline $U = 752.5$, $p = .97$; bupivacaine, $U = 687$, $p = .49$). An increase in both the number of timeouts to reach criterion (Figure 3c, Wilcoxon Signed-ranks test, DHC, $Z = -2.20$, $p = .03$; VHC, $Z = -3.06$, $p = .002$) and the total distance traveled by the rats before reaching the learning criterion (Figure 3e, Wilcoxon Signed-ranks test, DHC, $Z = -2.79$, $p = .005$; VHC, $Z = -3.06$, $p = .002$) were observed after bupivacaine infusion into the

DHC or VHC compared to saline. Additional analyses revealed that the effects of VHC inactivation were not significantly different from those observed with DHC inactivation for the number of timeouts (Mann–Whitney test, saline $U = 83.5$, $p = .98$; bupivacaine, $U = 77$, $p = .72$) or for the total distance traveled (Mann–Whitney test, saline $U = 68$, $p = .41$; bupivacaine, $U = 70$, $p = .47$). These results show that the temporary inactivation of DHC or VHC causes similar decreases in memory-guided spatial navigation performance in environments with large obstacles. This effect was not observed in obstacle-free environments (Figure 2).

3.4 | Experiment 3: effect of dorsal or ventral hippocampus inactivation on memory-guided navigation in environments with small obstacles

The involvement of VHC in spatial navigation in Experiment 2 may be due to the large scale of the obstacles. The purpose of this experiment was to evaluate the effect of DHC or VHC inactivation on memory-guided navigation in a more complex environment featuring many choice points that were due to the presence of small obstacles. As in Experiments 1 and 2, rats learned a spatial set of feeders in an obstacle-free environment before being infused with saline or bupivacaine into the DHC or VHC. They were then tested during recall in the presence of small obstacles. Figure 4a shows representative rat trajectories during recall in the small obstacle condition after bilateral saline or bupivacaine infusions into the DHC or VHC. The number of times rats stopped at nontarget feeders did not differ between saline and bupivacaine infusions into the DHC (Figure 4b, Wilcoxon Signed-ranks test, $Z = -1.60$, $p = .11$) but we found a significant effect in the VHC inactivation condition (Figure 4b, Wilcoxon Signed-ranks test, $Z = -2.04$, $p = .04$). There was no significant difference in the number of stops between DHC and VHC inactivation (Mann–Whitney test, saline $U = 46$, $p = .11$; bupivacaine, $U = 52.5$, $p = .27$). We also observed that the inactivation of VHC or DHC increased the number of timeouts to reach recall criterion (Figure 4c, Wilcoxon Signed-ranks test, DHC, $Z = -2.34$, $p = .02$; VHC, $Z = -2.47$, $p = .01$). There were also no significant differences between DHC and VHC inactivation using this measure (Mann–Whitney test, saline $U = 78.5$, $p = .78$; bupivacaine, $U = 67.5$, $p = .57$). Similarly, the inactivation of the VHC or DHC significantly increased the number of monotonous segments (Figure 4d, Wilcoxon Signed-ranks test, DHC, $Z = -2.03$, $p = .04$; VHC, $Z = -4.37$, $p = .00$), indicating a clear deficiency in navigating/turning around the small obstacles. Additional analyses showed that, unlike with the large obstacle condition, the effect of the VHC inactivation was significantly higher than that observed with DHC inactivation (Mann–Whitney test, saline $U = 673.5$, $p = .41$; bupivacaine, $U = 461$, $p = .005$). Finally, bupivacaine administration into the DHC or VHC significantly increased the total distance traveled by the rats before reaching the recall criterion (Figure 4e, Wilcoxon Signed-ranks test, DHC, $Z = -2.67$, $p = .008$; VHC, $Z = -2.67$, $p = .008$). There was no significant difference between the DHC and VHC groups (Mann–Whitney test, saline $U = 69$, $p = .44$; bupivacaine, $U = 58$, $p = .18$). These results show that the temporary inactivation of the DHC or VHC causes a decrease in performance in memory-guided spatial navigation in small obstacle-rich environments. The decrease in spatial performance was not due to a general motor impairment because no significant differences between saline and bupivacaine infusion were observed in velocity (Figure 5a, Wilcoxon Signed-ranks test, DHC, $Z = -1.13$, $p = .26$; VHC, $Z = -1.78$, $p = .08$) or average segment tortuosity (Figure 5b, Wilcoxon Signed-ranks test, DHC, $Z = -1.08$, $p = .28$; VHC, $Z = -0.56$, $p = .58$).

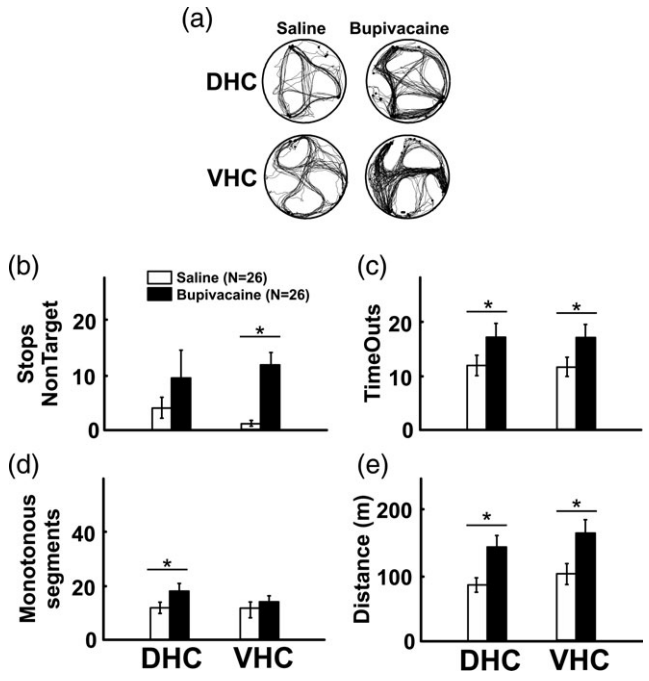

FIGURE 3 Spatial navigation in large obstacle-rich environments is impaired by VHC and DHC inactivation. (a) Representative rat trajectories during recall after saline or bupivacaine infusions in the DHC (upper) or VHC (lower). (b) Number of times rats stopped at nontargets. (c) Number of timeouts required to reach criterion. (d) Average number of monotonous segments. (e) Total distance traveled before reaching recall criterion. *N* indicates a number of sessions. DHC group, $n = 8$ rats. VHC group, $n = 9$ rats

3.5 | Maze complexity and navigation performance analyses

Linear regression was used to compare the relationship between navigation performance and maze complexity during recall. Fisher's *r*-to-*Z* tests were used to assess the statistical differences between saline and bupivacaine correlation coefficients. Figure 6 shows a schematic representation of the three proposed measures of maze complexity (see Methods). Figure 7 shows the linear regression analyses for the large obstacles condition. Statistically significant cases are indicated by gray shaded boxes. We observed that in the saline condition (DHC and VHC combined, white circles) the number of timeout light cues that were required to reach criterion was negatively correlated with obstacle density (Figure 7b, $r^2 = .24$, $F[1,26] = 8.31$, $p = .008$) and positively correlated with the straight-path complexity (Figure 7c, $r^2 = .29$, $F[1,26] = 10.55$, $p = .003$). There was no significant correlation between these maze complexity measures and the number of timeout light cues after bupivacaine injection (DHC and VHC combined, black circles; Figure 7b, density, $r^2 = .00$, $F[1,26] = 0.003$, $p = .96$; Figure 7c, straight-path complexity, $r^2 = .12$, $F[1,26] = 3.59$,

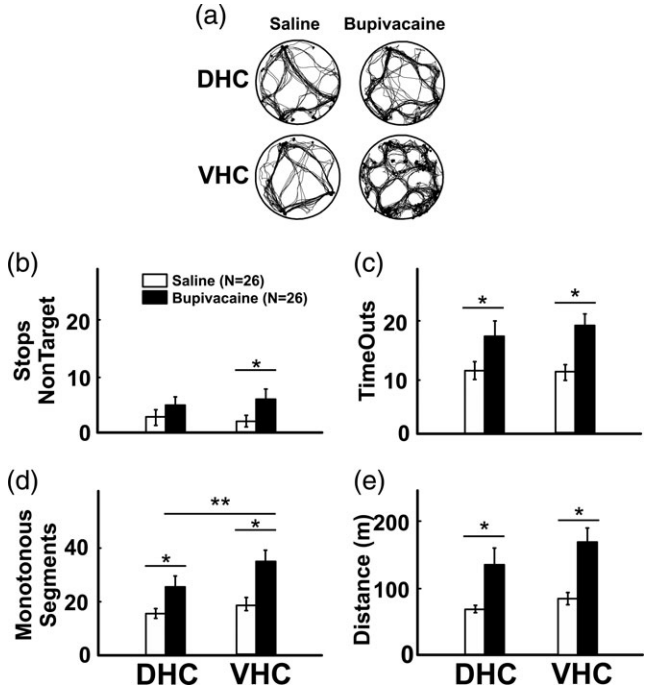

FIGURE 4 Inactivation of either the VHC or DHC impairs spatial navigation in small obstacle-rich environments. (a) Representative trajectories during recall after saline or bupivacaine infusion in the DHC (upper) or VHC (lower). (b) Number of times rats stopped at nontargets. (c) Number of timeouts required to reach criterion. (d) Average number of monotonous segments. (e) Total distance traveled before reaching recall criterion. *N* indicates a number of sessions. DHC group, *n* = 8 rats. VHC group, *n* = 9 rats

p = .07). We did not observe significant correlations between the number of timeout light cues and line-of-sight complexity (Figure 7a, saline, r^2 = .06, *F*[1,26] = 1.62, *p* = .21; bupivacaine, r^2 = .07, F [1,26] = 2.03, *p* = .17). No significant difference was found between saline and bupivacaine correlation coefficients (line-of-sight complexity, *Z* = −0.1, *p* = .99; density, *Z* = 1.87, *p* = .06; straight-path complexity, *Z* = 0.84, *p* = .40). We also observed that the number of monotonous segments was negatively correlated with both line-of-sight complexity (Figure 7a, r^2 = .46, *F*[1,26] = 8.48, *p* = .007) and density (Figure 7b, r^2 = .15, *F*[1,26] = 4.7, *p* = .039) in the saline condition. The number of monotonous segments was still negatively correlated with the line-of-sight complexity (Figure 7a, r^2 = .22, *F* [1,26] = 7.41, *p* = .011) but not with the density (Figure 7b, r^2 = .05, *F* [1,26] = 1.297, *p* = .265) after bupivacaine injection. There was no significant correlation between the number of monotonous segments and straight-path complexity (Figure 7c, saline, r^2 = .13, *F* (1,54) = 3.73, *p* = .06; bupivacaine, r^2 = .04, *F*(1,26) = 1.125, *p* = .299). No significant difference was found between saline and bupivacaine correlation coefficients (line-of-sight complexity, *Z* = 1.1, *p* = .90; density, *Z* = 0.68, *p* = .5; straight-path complexity, *Z* = 0.58, *p* = .56). A significant negative correlation was also found between the total distance traveled by the rats before reaching the recall criterion and the Density (Figure 7b, r^2 = .34, *F*(1,26) = 13.49, *p* = .001) after saline injection. We did not observe correlations between these two variables in the bupivacaine condition (Figure 7b, r^2 = .09, *F* (1,26) = 2.499, *p* = .125). We also did not observe correlations between this variable and the other two measures of the maze complexity in the saline or bupivacaine conditions (Figure 7a, line-of-sight complexity, saline, r^2 = .00, *F*(1,26) = 0.004, *p* = .949, bupivacaine, r^2 = .01, *F*(1,26) = 0.33, *p* = .57; Figure 7c, straight-path complexity, saline, r^2 = 0.07, *F*(1,26) = 2.08, *p* = .16, bupivacaine, r^2 = .01, *F* (1,26) = 0.016, *p* = .90). No significant difference was found between saline and bupivacaine correlation coefficients (line-of-sight complexity, *Z* = −0.35, *p* = .73; density, *Z* = 1.28, *p* = .2; straight-path complexity, *Z* = 0.63, *p* = .37). Finally, there was a negative correlation between the number of times rats stopped at nontarget feeders and the density in the saline (data not shown, r^2 = .29, *F*[1,25] = 10.13, *p* = .004), but not bupivacaine (data not shown, r^2 = .14, *F* [1,25] = 4.09, *p* = .054), condition. We did not observe correlations between this variable and the other two measures of the maze complexity in the saline or bupivacaine conditions (data not shown, line-of-sight complexity, saline, r^2 = .00, *F*(1,25) = 0.09, *p* = .92, bupivacaine, r^2 = .00, *F*(1,25) = 0.00, *p* = .99; straight-path complexity, saline, r^2 = 0.01, *F*(1,25) = 0.03, *p* = .86, bupivacaine, r^2 = 0.01, *F* (1,25) = 0.25, *p* = .62). No significant difference was found between saline and bupivacaine correlation coefficients (line-of-sight complexity, *Z* = −0.01, *p* = .99; density, *Z* = 0.73, *p* = .47; straight-path complexity, *Z* = −0.00, *p* = 1.0).

We found a negative correlation between the number of monotonous segments and the density after saline injection in the small obstacles condition (Figure 8b, r^2 = .17, *F*(1,26) = 5.37, *p* = .029). These two variables remained correlated during bupivacaine conditions (Figure 8b, r^2 = .18, *F*(1,26) = 5.51, *p* = .027). During HC inactivation, the number of monotonous segments (Figure 8a, saline, r^2 = .02, *F*(1,26) = 0.56, *p* = .46, bupivacaine, r^2 = .25, *F*(1,26) = 8.44, *p* = .007) and the number of timeouts (Figure 8a, saline, r^2 = .12, *F* (1,26) = 3.498, *p* = .07, bupivacaine, r^2 = .15, *F*(1,25) = 4.28, *p* = .049) were negatively correlated with line-of-sight complexity. There was no significant correlation between the number of monotonous segments and straight-path complexity (Figure 8c, saline, r^2 = .01, *F* (1,26) = 0.03, *p* = .85; bupivacaine, r^2 = .11, *F*(1,26) = 3.06, *p* = .09). We did not observe correlations between number of timeouts and the other two measures of the maze complexity in the saline or bupivacaine conditions (Figure 8b, density, saline, r^2 = 0.01, *F*(1,26) = 0.03, *p* = .86, bupivacaine, r^2 = 0.03, *F*(1,25) = 0.87, *p* = .36; Figure 8c, straight-path complexity, saline, r^2 = .00, *F*(1,26) = 0.004, *p* = .95; bupivacaine, r^2 = .001, *F*(1,25) = 0.013, *p* = .91). No significant differences were found between saline and bupivacaine correlation

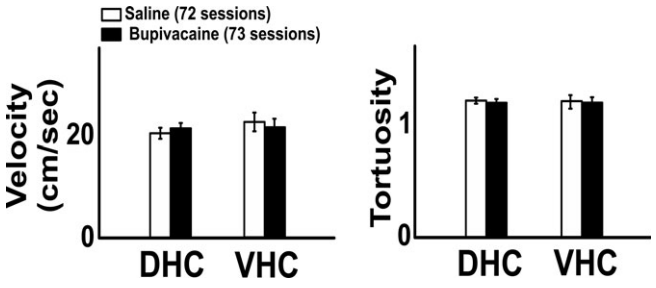

FIGURE 5 Inactivation of the VHC or DHC does not affect the rat's overall movement. (a) Velocity and (b) path tortuosity. N indicates a number of sessions. DHC group, *n* = 8 rats. VHC group, *n* = 9 rats

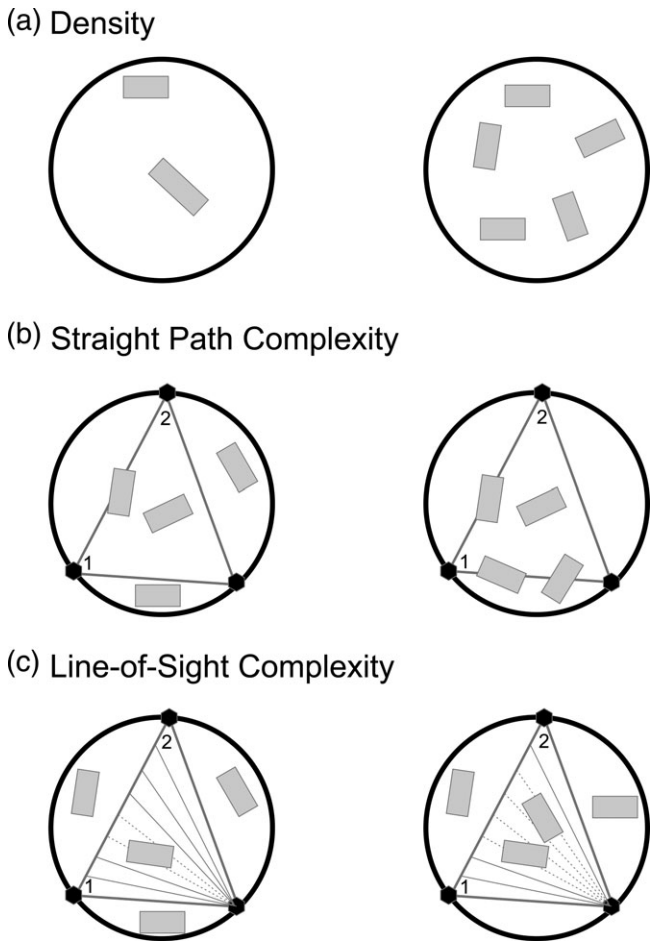

FIGURE 6 Measures of maze complexity. (a) Left: low obstacle density, right: high obstacle density. (b) Left: one obstacle on straight paths. Right: three obstacles on straight paths. (c) Line-of-sight complexity for segment 1–2, for an 8-segment discretization. Two obstructions are found (dashed lines). Right: four obstructions are found in this configuration

coefficients (Monotonous segments, line-of-sight complexity, $Z = -1.4$, $p = .16$; Density, $Z = -0.02$, $p = .98$; straight-path complexity, $Z = -1.16$, $p = .32$; timeouts, line-of-sight complexity, $Z = -0.15$, $p = .88$; density, $Z = -0.30$, $p = .8$; straight-path complexity, $Z = -0.04$, $p = .97$). Finally, there was no significant correlation between the total distance traveled (Figures 8a,c, line-of-sight complexity, saline, $r^2 = .03$, $F(1,26) = 0.69$, $p = .41$, bupivacaine, $r^2 = .06$, $F(1,26) = 1.65$, $p = .21$; density, saline, $r^2 = .11$, $F(1,26) = 3.29$, $p = .08$, bupivacaine, $r^2 = 0.03$, $F(1,26) = 0.77$, $p = .39$; straight-path complexity, saline, $r^2 = .01$, $F(1,26) = 0.18$, $p = .66$, bupivacaine, $r^2 = .001$, $F(1,26) = 0.03$, $p = .87$) or the number of times rats stopped at nontarget feeders (data not shown, line-of-sight complexity, saline, $r^2 = .01$, $F(1,26) = 0.20$, $p = .66$, bupivacaine, $r^2 = .03$, $F(1,26) = 0.71$, $p = .41$; density, saline, $r^2 = .01$, $F(1,26) = 0.22$, $p = .65$, bupivacaine, $r^2 = .02$, $F(1,26) = 0.48$, $p = .49$; straight-path complexity, saline, $r^2 = .09$, $F(1,26) = 2.5$, $p = .13$, bupivacaine, $r^2 = .01$, $F(1,26) = 0.34$, $p = .57$) with the different measures of the maze complexity in the saline or bupivacaine conditions. No significant difference was found between saline and bupivacaine correlation coefficients (distance traveled, line-of-sight complexity, $Z = -0.3$, $p = .76$; density, $Z = 0.63$, $p = .53$; straight-path complexity, $Z = 0.19$, $p = .85$; stops nontarget feeders, line-of-sight complexity, $Z = -0.27$, $p = .79$; density, $Z = -0.16$, $p = .87$; straight-path complexity, $Z = 0.68$, $p = .50$).

In sum, these results indicate that in the saline conditions, the navigation performance during recall was highly correlated with the complexity of the maze, mainly in the large, but not in the small, obstacles conditions. The statistical significance of the relationships between navigation and maze complexity were affected by the inactivation of either the dorsal or ventral hippocampal divisions. This finding shows that both DHC and VHC are involved in spatial navigation in complex (large obstacles) environments.

4 | DISCUSSION

Our results show that navigation in complex obstacle-rich spatial environments involves both the dorsal and ventral portions of the hippocampus. We found that inactivation of the DHC and VHC impaired memory driven navigation in environments featuring obstacle-induced choice points (Figures 3 and 4). We also found that in a simple environment (no obstacles) the inactivation of these hippocampal regions did not affect spatial memory performance (Figure 2), suggesting that the effect observed was due to the presence of obstacles, not to the parameters of the injections (Figure 5). Furthermore, the regression analyses between maze complexity and navigational performance showed clear co-variations in the large obstacles condition (Figure 7), suggesting that it represented a more complex spatial layout than with small obstacles (Figure 8). The overall findings of this study suggest that goal-directed navigation in a complex environment requires a greater involvement of the hippocampal circuitry than previously thought, including at the ventral levels.

Goal-directed navigation requires the concerted action of multiple brain regions that are known to be involved in spatial representation, planning, learning, and memory (Pezzulo, van der Meer, Lansink, & Pennartz, 2014; Verschure, Pennartz, & Pezzulo, 2014). The finding that the inactivation of the DHC impaired spatial navigation in complex environments is broadly compatible with numerous studies showing that the DHC is necessary for spatial learning and navigation in obstacle-free environments (Harland et al., 2017). For instance, rats with lesions or inactivation of the DHC showed a marked deficit in spatial learning in the water maze (Moser et al., 1993; Moser, Moser, Forrest, Andersen, & Morris, 1995; Riedel et al., 1999) or honeycomb maze (Wood et al., 2018). Further support for the relevance of the DHC in spatial learning comes from genetic manipulation studies in which the disruption of transcription factors that are important for long-term memory formation in the dorsal CA1 impaired learning in the water maze (Pittenger et al., 2002). Similarly, DHC lesions impaired spatial performance on working memory tasks (Bannerman et al., 2002). The DHC contains place cells with small and spatially selective place fields (Jung et al., 1994) suggesting that the dorsal pole may store a detailed spatial representation of the environment.

Although several studies have shown that VHC manipulations did not impair spatial learning in simple obstacles-free environments such as the water maze (Moser et al., 1993; Moser et al., 1995), radial-arm maze (Pothuizen, Zhang, Jongen-Relo, Feldon, & Yee, 2004) and

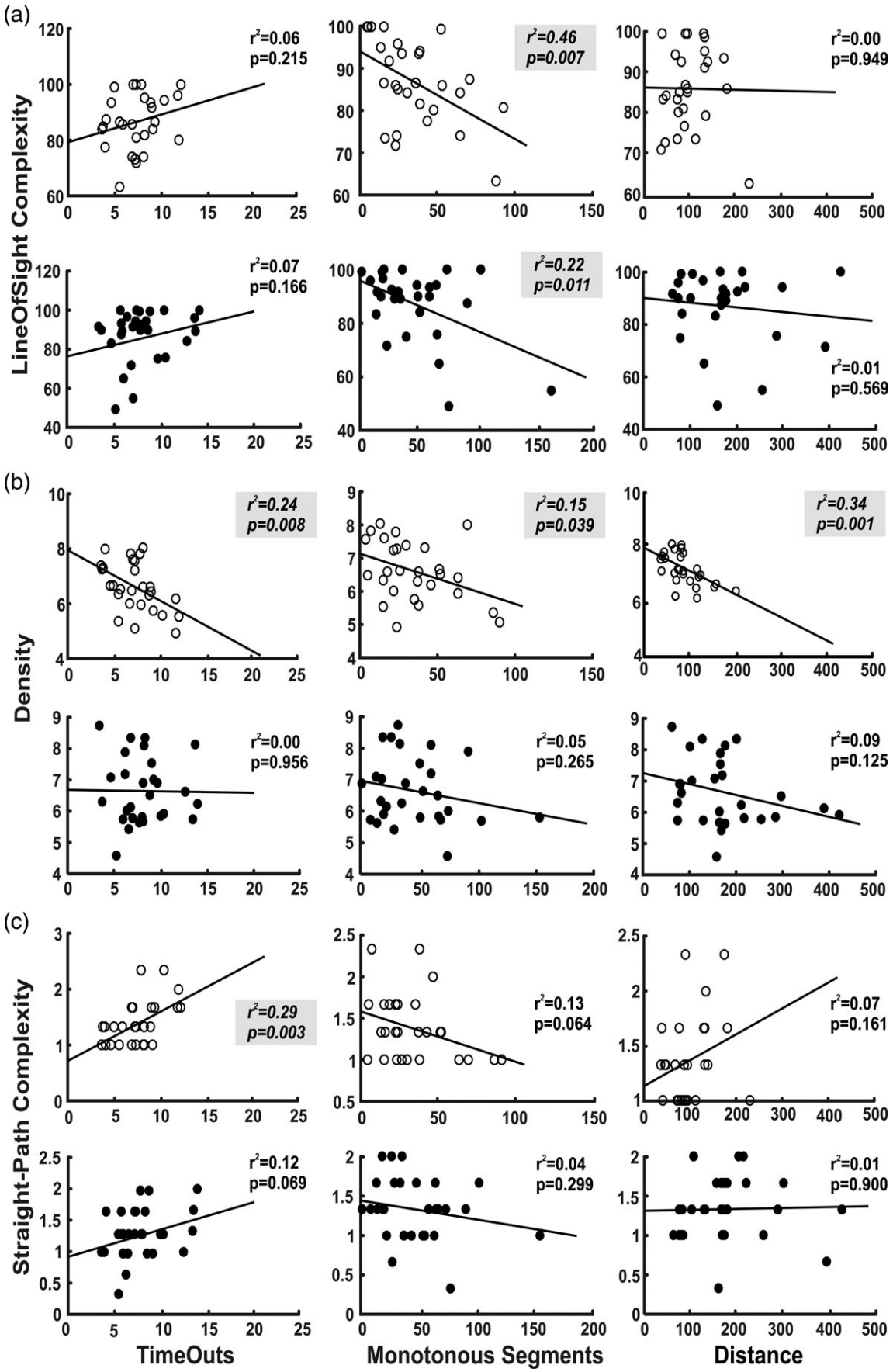

FIGURE 7 Relationships between navigational performance and maze complexity in large obstacles condition. Linear regression lines and coefficients of determination values are indicated. Saline injections in the DHC or VHC (N = 26) are represented by white circles and bupivacaine injections (N = 26) by black circles. (a): Line-of-sight complexity. (b) Density. (c): Straight-path complexity

T-maze (Potvin, Allen, Thibaudeau, Dore, & Goulet, 2006), evidence from other studies appear to be inconsistent with the hypothesis that VHC is not involved in spatial navigation. Indeed, previous work has shown that VHC lesions impaired spatial learning in the water maze when the position of the submerged platform was varied during each session (Ferbinteanu et al., 2003). Others also showed that posttraining VHC lesions affected the ability to learn the position of the submerged platform in a novel environment (de Hoz & Martin, 2014). In addition, the reversible inactivation of the VHC delivered just before the beginning of a probe trial in a water maze task produced a memory retrieval deficit (Loureiro et al., 2012), and others showed that the VHC was primarily involved in the initial stages of trial-and-error learning in the water maze (Ruediger et al., 2012). We found that the inactivation of the VHC leads to the visits of nonrewarded feeders (nontargets), irrespective of obstacle size. This result is compatible with the known anatomical connections between VHC and planning and reward-processing areas such as mPFC, striatum or the VTA. Our finding that the inactivation of the VHC impaired navigation in obstacle-rich environment is consistent with these studies and strongly suggests the unifying theory that the ventral pole of the HC, which is traditionally thought to be involved in emotional and motivational processes (Fanselow & Dong, 2010) may play a prominent role in goal-directed navigation in complex environments.

An additional difficulty in interpreting the involvement of the VHC in the water maze task is that the task includes an intrinsic anxiogenic component due to forced swimming. It is well documented that lesions or reversible inactivations of the VHC impair fear learning and anxiety responses (Adhikari, Topiwala, & Gordon, 2010; Bannerman et al., 2003; Trivedi & Coover, 2004). In our study, we used a positively motivated spatial task (Adhikari et al., 2010; Bannerman et al., 2003; Jones et al., 2012; Trivedi & Coover, 2004) that lacks this stress component, and therefore suggests that the deficit in navigation seen after the VHC inactivation was likely, not due to an altered emotional responses during the recall phase. Our results point to a failure to combine the coarse information encoded by VHC with more detailed DHC spatial information necessary to form the type of integrated multiscale spatial representations that may be necessary for complex, obstacle-rich environments. We hypothesized that the increase in cognitive demands due to the presence of obstacles during recall required the interactions of spatial maps at multiple scales along the dorsoventral axis of the HC. We also suggest that whereas spatial processing invariably involves the activation of the DHC, the VHC becomes involved only when more complex spatial processing is required. In support of this idea, it has been reported in humans, that the level of complexity of a virtual environment (number of distinct possible paths) engaged the anterior part (rodents VHC), but not posterior segment (rodents DHC) of the hippocampus. In contrast, variation in the size of the environments engaged the posterior, but not anterior hippocampus (Baumann & Mattingley, 2013). In our study, a stronger relationship between navigational performance and complexity was found in the large obstacles condition, suggesting that large obstacles resulted in a more challenging spatial navigation than small obstacles. This finding may be explained by the fact that in the presence of large obstacles, animals were forced to do major modifications to their trajectories, likely involving more planning and decision making, to reach the reward locations.

Differences in spatial coding have been observed along the longitudinal axis of the HC. Ventral place cells were less common and had larger and less spatially selective place fields than dorsal place cells (Jung et al., 1994; Kjelstrup et al., 2008), nevertheless, it has been also shown that the spatial resolution represented by population of ventral CA1 cells was comparable to that of DHC (Keinath et al., 2014). The gradient of place field size along the longitudinal hippocampal axis may signal a shift from sparse to distributed coding rather than a loss of spatial resolution and may in addition suggest a role for ventral cells in spatial context processing and generalization (Evensmoen et al., 2015; Keinath et al., 2014; Nadel, Hoscheidt, & Ryan, 2013). This previous work, and our result, together point to a functional organization of the hippocampal long axis in which a smooth gradient of place field size implements a representation of space at multiple scales and levels of detail (Geva-Sagiv, Las, Yovel, & Ulanovsky, 2015).

Flexible navigation in complex environments is likely supported by a multiscale memory system in the hippocampus and associated structures (Geva-Sagiv et al., 2015). For instance, situations in which the animal needs to compute more efficient navigational paths toward a goal or has to learn about changes in the environmental context or size are likely to require more spatial processing and planning. In our study, obstacles prevented the direct perception of the goal locations, forcing the animals to plan complex routes featuring a large number of decision points, particularly, in the large obstacles conditions. The presence of such obstructions during recall makes it unlikely that the environment can be encoded using a single reference frame (Wolbers & Wiener, 2014). Instead, these representations are likely fragmented into overlapping units, which are then coarsely integrated and used for complex navigation. The simultaneous encoding of space at different scales along the long axis of the HC may be one of the computational advantages that allow for such fragmentation/integration to occur on demand (Harland et al., 2017). The spatial representations of obstacle-rich environments may be a collection of smaller detailed DHC spatial maps linked together by a coarser more global representation involving the VHC levels. Importantly, our data showed that, in the conditions of our injections, the inactivation of VHC or DHC during obstacle-free recall sessions did not impair spatial navigation suggesting that memory-guided navigation in simple spatial environments, where the goal location is visible from any position in the maze, may not have required a strong coordination along the dorsoventral hippocampal axis. In addition, these results may also suggest that in the inactivation conditions of our study, either one of DHC or VHC was sufficient to support correct recall in simple environments.

Spatial navigation is thought to rely on at least two major components (Moser et al., 2014). The first is path integration (egocentric strategy), with which the animal uses proprioceptive and self-motion information to estimate displacement, and the second is sensory driven navigation (allocentric strategy) whereby visual (or other modality) features of the environment determine the manner in which neurons encode the absolute location of the animal in space. In our

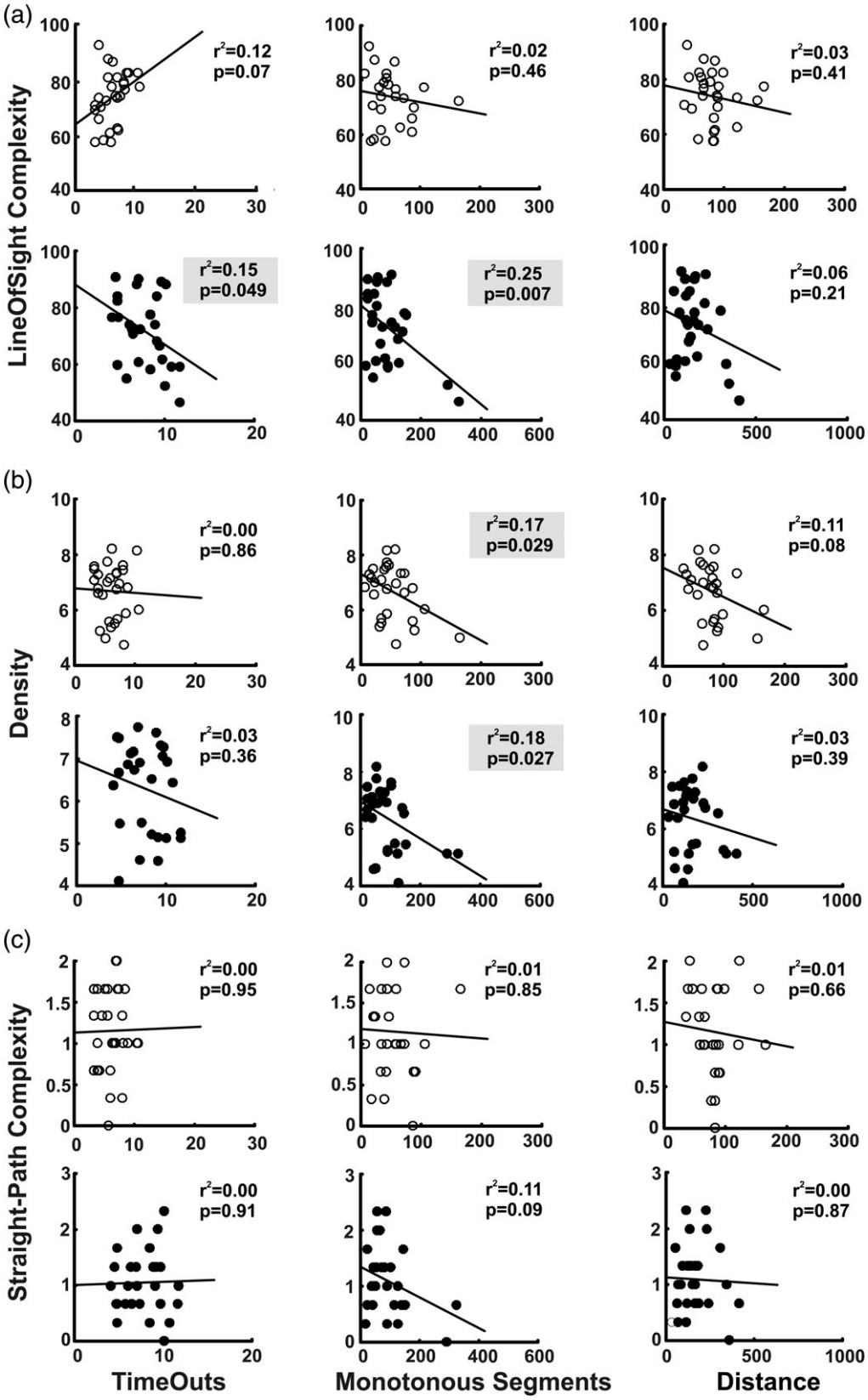

FIGURE 8 Relationships between navigational performance and maze complexity in small obstacles condition. Linear regression lines and coefficients of determination values are indicated. Saline injections in the DHC or VHC (N = 26) are represented by white circles and bupivacaine injections (N = 26) by black circles. (a): Line-of-sight complexity. (b) Density. (c) Straight-path complexity

study, the navigation toward the goal in obstacle-rich environments likely involved allocentric strategies (in addition to path integration strategies), because it required path planning and navigation on novel routes around mostly unexpected obstacles (wayfinding). Studies in human navigating a virtual maze have shown that the posterior HC was involved in accurate navigation in which goal locations needed to

be computed dynamically, as in our obstacle-rich conditions (Hartley, Maguire, Spiers, & Burgess, 2003). A recent study showed that the anterior HC was strongly involved when approaching a goal location, suggesting that this portion of the structure might be involved in non-spatial signals, such as reward expectation (Viard, Doeller, Hartley, Bird, & Burgess, 2011). A similar result was found in rats when different subpopulations of ventral CA1 neurons increased or decreased their firing as the animals approached a reward zone (Ciocchi et al., 2015).

Recent optogenetic studies in rodents have demonstrated that the HC was involved in navigational planning (Miller, Botvinick, & Brody, 2017) and goal-directed navigation (Ciocchi et al., 2015; de Lavilleon, Lacroix, Rondi-Reig, & Benchenane, 2015; Ito, Zhang, Witter, Moser, & Moser, 2015). In addition, dorsal CA1 place cells generated brief sequences (replay) encoding spatial trajectories which seems to support a goal-directed, trajectory-finding mechanism (Pfeiffer & Foster, 2013), and the activity of the neural ensembles from the dorsal CA3 region have been associated with decision making (Johnson & Redish, 2007). Little is known however about VHC replay or the role of VHC in decision-making.

Finally, it is worth considering that the introduction of obstacles into a familiar environment during recall may have engaged the working memory system in addition to the spatial navigation system. Since the obstacles interrupt the intended navigational paths, rats had to memorize the location of the goal, then devise subpaths aimed at contouring the obstacles. As such, the behavior was likely to engage working memory circuitry including that of the mPFC and circuitry involved in transitive inferences. Both DHC (Bannerman et al., 2002) and VHC (Hall et al., 2017) have been involved in working memory tasks in rodents. Interestingly, the VHC (or anterior in human) has been shown to be primarily involved in transitive inferences, albeit in nonspatial tasks (Bunsey & Eichenbaum, 1996; Heckers, Zalesak, Weiss, Ditman, & Titone, 2004).

Together, these data suggest that spatial navigation in complex environments may involve the entire extent of the longitudinal axis of the hippocampus. The VHC involvement in spatial navigation seen in our study may be explained, at least in part, by the need for more complex spatial processing associated with the presence of obstacles during the recall. Further studies are necessary to understand the role of the longitudinal axis of the HC in goal-directed spatial navigation tasks in complex and large-scale environments.

ACKNOWLEDGMENTS

The authors thank the members of the Computational and Experimental Neuroscience Laboratory for all their help.

ORCID

Martin Llofriu http://orcid.org/0000-0003-1302-3394
Jean-Marc Fellous http://orcid.org/0000-0003-4102-8336

REFERENCES

Adhikari, A., Topiwala, M. A., & Gordon, J. A. (2010). Synchronized activity between the ventral hippocampus and the medial prefrontal cortex during anxiety. *Neuron*, *65*(2), 257–269.

Amaral, D. G., & Kurz, J. (1985). An analysis of the origins of the cholinergic and noncholinergic septal projections to the hippocampal formation of the rat. *The Journal of Comparative Neurology*, *240*(1), 37–59.

Bannerman, D. M., Deacon, R. M., Offen, S., Friswell, J., Grubb, M., & Rawlins, J. N. (2002). Double dissociation of function within the hippocampus: Spatial memory and hyponeophagia. *Behavioral Neuroscience*, *116*(5), 884–901.

Bannerman, D. M., Grubb, M., Deacon, R. M., Yee, B. K., Feldon, J., & Rawlins, J. N. (2003). Ventral hippocampal lesions affect anxiety but not spatial learning. *Behavioural Brain Research*, *139*(1–2), 197–213.

Bast, T., Wilson, I. A., Witter, M. P., & Morris, R. G. (2009). From rapid place learning to behavioral performance: A key role for the intermediate hippocampus. *PLoS Biology*, *7*(4), e1000089.

Baumann, O., & Mattingley, J. B. (2013). Dissociable representations of environmental size and complexity in the human hippocampus. *The Journal of Neuroscience*, *33*(25), 10526–10533.

Bunsey, M., & Eichenbaum, H. (1996). Conservation of hippocampal memory function in rats and humans. *Nature*, *379*(6562), 255–257.

Callaway, J. K., Jones, N. C., & Royse, C. F. (2012). Isoflurane induces cognitive deficits in the Morris water maze task in rats. *European Journal of Anaesthesiology*, *29*(5), 239–245.

Carr, Z. J., Torjman, M. C., Manu, K., Dy, G., & Goldberg, M. E. (2011). Spatial memory using active allothetic place avoidance in adult rats after isoflurane anesthesia: A potential model for postoperative cognitive dysfunction. *Journal of Neurosurgical Anesthesiology*, *23*(2), 138–145.

Ciocchi, S., Passecker, J., Malagon-Vina, H., Mikus, N., & Klausberger, T. (2015). Brain computation. Selective information routing by ventral hippocampal CA1 projection neurons. *Science*, *348*(6234), 560–563.

de Hoz, L., Knox, J., & Morris, R. G. (2003). Longitudinal axis of the hippocampus: Both septal and temporal poles of the hippocampus support water maze spatial learning depending on the training protocol. *Hippocampus*, *13*(5), 587–603.

de Hoz, L., & Martin, S. J. (2014). Double dissociation between the contributions of the septal and temporal hippocampus to spatial learning: The role of prior experience. *Hippocampus*, *24*(8), 990–1005.

de Lavilleon, G., Lacroix, M. M., Rondi-Reig, L., & Benchenane, K. (2015). Explicit memory creation during sleep demonstrates a causal role of place cells in navigation. *Nature Neuroscience*, *18*(4), 493–495.

De Saint, B. P., Hok, V., Save, E., Poucet, B., & Chaillan, F. A. (2013). Differential role of the dorsal hippocampus, ventro-intermediate hippocampus, and medial prefrontal cortex in updating the value of a spatial goal. *Hippocampus*, *23*(5), 342–351.

Deacon, R. M., Bannerman, D. M., & Rawlins, J. N. (2002). Anxiolytic effects of cytotoxic hippocampal lesions in rats. *Behavioral Neuroscience*, *116*(3), 494–497.

Dougherty, K. A., Islam, T., & Johnston, D. (2012). Intrinsic excitability of CA1 pyramidal neurones from the rat dorsal and ventral hippocampus. *The Journal of Physiology*, *590*(Pt 22), 5707–5722.

Edeline, J. M., Hars, B., Hennevin, E., & Cotillon, N. (2002). Muscimol diffusion after intracerebral microinjections: A reevaluation based on electrophysiological and autoradiographic quantifications. *Neurobiology of Learning and Memory*, *78*(1), 100–124.

Evensmoen, H. R., Ladstein, J., Hansen, T. I., Moller, J. A., Witter, M. P., Nadel, L., & Haberg, A. K. (2015). From details to large scale: The representation of environmental positions follows a granularity gradient along the human hippocampal and entorhinal anterior-posterior axis. *Hippocampus*, *25*(1), 119–135.

Fanselow, M. S., & Dong, H. W. (2010). Are the dorsal and ventral hippocampus functionally distinct structures? *Neuron*, *65*(1), 7–19.

Farnham, M. M., & Pilowsky, P. M. (2009). Local anaesthetics for acute reversible blockade of the sympathetic baroreceptor reflex in the rat. *Journal of Neuroscience Methods*, *179*(1), 58–62.

Ferbinteanu, J., Ray, C., & McDonald, R. J. (2003). Both dorsal and ventral hippocampus contribute to spatial learning in long-Evans rats. *Neuroscience Letters*, *345*(2), 131–135.

Gabriele, A., & Packard, M. G. (2006). Evidence of a role for multiple memory systems in behavioral extinction. *Neurobiology of Learning and Memory*, *85*(3), 289–299.

Gasbarri, A., Verney, C., Innocenzi, R., Campana, E., & Pacitti, C. (1994). Mesolimbic dopaminergic neurons innervating the hippocampal formation in the rat: A combined retrograde tracing and immunohistochemical study. *Brain Research*, *668*(1–2), 71–79.

Gaskin, S., Gamliel, A., Tardif, M., Cole, E., & Mumby, D. G. (2009). Incidental (unreinforced) and reinforced spatial learning in rats with ventral and dorsal lesions of the hippocampus. *Behavioural Brain Research*, *202*(1), 64–70.

Geva-Sagiv, M., Las, L., Yovel, Y., & Ulanovsky, N. (2015). Spatial cognition in bats and rats: From sensory acquisition to multiscale maps and navigation. *Nature Reviews. Neuroscience*, *16*(2), 94–108.

Giocomo, L. M., & Hasselmo, M. E. (2008). Time constants of h current in layer ii stellate cells differ along the dorsal to ventral axis of medial entorhinal cortex. *The Journal of Neuroscience*, *28*(38), 9414–9425.

Giocomo, L. M., & Hasselmo, M. E. (2009). Knock-out of HCN1 subunit flattens dorsal-ventral frequency gradient of medial entorhinal neurons in adult mice. *The Journal of Neuroscience*, *29*(23), 7625–7630.

Hall, B. J., Abreu-Villaca, Y., Cauley, M., Junaid, S., White, H., Kiany, A., & Levin, E. D. (2017). The ventral hippocampal muscarinic cholinergic system plays a key role in sexual dimorphisms of spatial working memory in rats. *Neuropharmacology*, *117*, 106–113.

Harland, B., Contreras, M., & Fellous, J. (2017). *A role for the longitudinal Axis of the hippocampus in multiscale representations of large and complex spatial environments and mnemonic hierarchies*. In: Stuchlik A, editor. Hippocampus.

Hartley, T., Maguire, E. A., Spiers, H. J., & Burgess, N. (2003). The well-worn route and the path less traveled: Distinct neural bases of route following and wayfinding in humans. *Neuron*, *37*(5), 877–888.

Heckers, S., Zalesak, M., Weiss, A. P., Ditman, T., & Titone, D. (2004). Hippocampal activation during transitive inference in humans. *Hippocampus*, *14*(2), 153–162.

Hok, V., Chah, E., Save, E., & Poucet, B. (2013). Prefrontal cortex focally modulates hippocampal place cell firing patterns. *The Journal of Neuroscience*, *33*(8), 3443–3451.

Ito, H. T., Zhang, S. J., Witter, M. P., Moser, E. I., & Moser, M. B. (2015). A prefrontal-thalamo-hippocampal circuit for goal-directed spatial navigation. *Nature*, *522*(7554), 50–55.

Johnson, A., & Redish, A. D. (2007). Neural ensembles in CA3 transiently encode paths forward of the animal at a decision point. *The Journal of Neuroscience*, *27*(45), 12176–12189.

Jones, B., Bukoski, E., Nadel, L., & Fellous, J. M. (2012). Remaking memories: Reconsolidation updates positively motivated spatial memory in rats. *Learning & Memory*, *19*(3), 91–98.

Jones, B. J., Pest, S. M., Vargas, I. M., Glisky, E. L., & Fellous, J. M. (2015). Contextual reminders fail to trigger memory reconsolidation in aged rats and aged humans. *Neurobiology of Learning and Memory*, *120*, 7–15.

Jung, M. W., Wiener, S. I., & McNaughton, B. L. (1994). Comparison of spatial firing characteristics of units in dorsal and ventral hippocampus of the rat. *The Journal of Neuroscience*, *14*(12), 7347–7356.

Keinath, A. T., Wang, M. E., Wann, E. G., Yuan, R. K., Dudman, J. T., & Muzzio, I. A. (2014). Precise spatial coding is preserved along the longitudinal hippocampal axis. *Hippocampus*, *24*(12), 1533–1548.

Kerr, K. M., Agster, K. L., Furtak, S. C., & Burwell, R. D. (2007). Functional neuroanatomy of the parahippocampal region: The lateral and medial entorhinal areas. *Hippocampus*, *17*(9), 697–708.

Kjelstrup, K. B., Solstad, T., Brun, V. H., Hafting, T., Leutgeb, S., Witter, M. P., … Moser, M. B. (2008). Finite scale of spatial representation in the hippocampus. *Science*, *321*(5885), 140–143.

Loureiro, M., Lecourtier, L., Engeln, M., Lopez, J., Cosquer, B., Geiger, K., … Pereira de Vasconcelos, A. (2012). The ventral hippocampus is necessary for expressing a spatial memory. *Brain Structure & Function*, *217*(1), 93–106.

Maurer, A. P., Vanrhoads, S. R., Sutherland, G. R., Lipa, P., & McNaughton, B. L. (2005). Self-motion and the origin of differential spatial scaling along the septo-temporal axis of the hippocampus. *Hippocampus*, *15*(7), 841–852.

Miller, K. J., Botvinick, M. M., & Brody, C. D. (2017). Dorsal hippocampus contributes to model-based planning. *Nature Neuroscience*, *20*, 1269–1276.

Moser, E., Moser, M. B., & Andersen, P. (1993). Spatial learning impairment parallels the magnitude of dorsal hippocampal lesions, but is hardly present following ventral lesions. *The Journal of Neuroscience*, *13*(9), 3916–3925.

Moser, E. I., Roudi, Y., Witter, M. P., Kentros, C., Bonhoeffer, T., & Moser, M. B. (2014). Grid cells and cortical representation. *Nature Reviews. Neuroscience*, *15*(7), 466–481.

Moser, M. B., Moser, E. I., Forrest, E., Andersen, P., & Morris, R. G. (1995). Spatial learning with a minislab in the dorsal hippocampus. *Proceedings of the National Academy of Sciences of the United States of America*, *92*(21), 9697–9701.

Nadel, L. (1968). Dorsal and ventral hippocampal lesions and behavior. *Physiology and Behavior*, *3*, 891–900.

Nadel, L., Hoscheidt, S., & Ryan, L. R. (2013). Spatial cognition and the hippocampus: The anterior-posterior axis. *Journal of Cognitive Neuroscience*, *25*(1), 22–28.

Pezzulo, G., van der Meer, M. A., Lansink, C. S., & Pennartz, C. M. (2014). Internally generated sequences in learning and executing goal-directed behavior. *Trends in Cognitive Sciences*, *18*(12), 647–657.

Pfeiffer, B. E., & Foster, D. J. (2013). Hippocampal place-cell sequences depict future paths to remembered goals. *Nature*, *497*(7447), 74–79.

Pittenger, C., Huang, Y. Y., Paletzki, R. F., Bourtchouladze, R., Scanlin, H., Vronskaya, S., & Kandel, E. R. (2002). Reversible inhibition of CREB/ATF transcription factors in region CA1 of the dorsal hippocampus disrupts hippocampus-dependent spatial memory. *Neuron*, *34*(3), 447–462.

Poppenk, J., Evensmoen, H. R., Moscovitch, M., & Nadel, L. (2013). Long-axis specialization of the human hippocampus. *Trends in Cognitive Sciences*, *17*(5), 230–240.

Pothuizen, H. H., Zhang, W. N., Jongen-Relo, A. L., Feldon, J., & Yee, B. K. (2004). Dissociation of function between the dorsal and the ventral hippocampus in spatial learning abilities of the rat: A within-subject, within-task comparison of reference and working spatial memory. *The European Journal of Neuroscience*, *19*(3), 705–712.

Potvin, O., Allen, K., Thibaudeau, G., Dore, F. Y., & Goulet, S. (2006). Performance on spatial working memory tasks after dorsal or ventral hippocampal lesions and adjacent damage to the subiculum. *Behavioral Neuroscience*, *120*(2), 413–422.

Richmond, M. A., Yee, B. K., Pouzet, B., Veenman, L., Rawlins, J. N., Feldon, J., & Bannerman, D. M. (1999). Dissociating context and space within the hippocampus: Effects of complete, dorsal, and ventral excitotoxic hippocampal lesions on conditioned freezing and spatial learning. *Behavioral Neuroscience*, *113*(6), 1189–1203.

Riedel, G., Micheau, J., Lam, A. G., Roloff, E. L., Martin, S. J., Bridge, H., … Morris, R. G. (1999). Reversible neural inactivation reveals hippocampal participation in several memory processes. *Nature Neuroscience*, *2*(10), 898–905.

Risold, P. Y., & Swanson, L. W. (1996). Structural evidence for functional domains in the rat hippocampus. *Science*, *272*(5267), 1484–1486.

Ruediger, S., Spirig, D., Donato, F., & Caroni, P. (2012). Goal-oriented searching mediated by ventral hippocampus early in trial-and-error learning. *Nature Neuroscience*, *15*(11), 1563–1571.

Schroeder, J. P., Wingard, J. C., & Packard, M. G. (2002). Post-training reversible inactivation of hippocampus reveals interference between memory systems. *Hippocampus*, *12*(2), 280–284.

Strange, B. A., Witter, M. P., Lein, E. S., & Moser, E. I. (2014). Functional organization of the hippocampal longitudinal axis. *Nature Reviews. Neuroscience*, *15*(10), 655–669.

Tehovnik, E. J., & Sommer, M. A. (1997). Effective spread and timecourse of neural inactivation caused by lidocaine injection in monkey cerebral cortex. *Journal of Neuroscience Methods*, *74*(1), 17–26.

Thompson, C. L., Pathak, S. D., Jeromin, A., Ng, L. L., MacPherson, C. R., Mortrud, M. T., … Lein, E. S. (2008). Genomic anatomy of the hippocampus. *Neuron*, *60*(6), 1010–1021.

Trivedi, M. A., & Coover, G. D. (2004). Lesions of the ventral hippocampus, but not the dorsal hippocampus, impair conditioned fear expression and inhibitory avoidance on the elevated T-maze. *Neurobiology of Learning and Memory*, *81*(3), 172–184.

Verschure, P. F., Pennartz, C. M., & Pezzulo, G. (2014). The why, what, where, when and how of goal-directed choice: Neuronal and computational principles. *Philosophical Transactions of the Royal Society of London. Series B, Biological Sciences*, *369*(1655), 20130483.

Viard, A., Doeller, C. F., Hartley, T., Bird, C. M., & Burgess, N. (2011). Anterior hippocampus and goal-directed spatial decision making. *The Journal of Neuroscience*, *31*(12), 4613–4621.

Wolbers, T., & Wiener, J. M. (2014). Challenges for identifying the neural mechanisms that support spatial navigation: The impact of spatial scale. *Frontiers in Human Neuroscience*, *8*, 571.

Wood, R. A., Bauza, M., Krupic, J., Burton, S., Delekate, A., Chan, D., & O'Keefe, J. (2018). The honeycomb maze provides a novel test to study hippocampal-dependent spatial navigation. *Nature*, *554*(7690), 102–105.

How to cite this article: Contreras M, Pelc T, Llofriu M, Weitzenfeld A, Fellous J-M. The ventral hippocampus is involved in multi-goal obstacle-rich spatial navigation. *Hippocampus*. 2018;1–14. https://doi.org/10.1002/hipo.22993